Stem Cell Reviews and Reports (2018) 14:812–822
https://doi.org/10.1007/s12015-018-9846-5

Endothelial Colony-Forming Cells Do Not Participate to Fibrogenesis in a Bleomycin-Induced Pulmonary Fibrosis Model in Nude Mice

Adeline Blandinières[1,2,3] · Thomas Gille[4] · Jérémy Sadoine[5] · Ivan Bièche[2,6] · Lofti Slimani[5] · Blandine Dizier[2,3] · Pascale Gaussem[1,2,3] · Catherine Chaussain[5] · Carole Planes[4] · Peter Dorfmüller[7] · Dominique Israël-Biet[2,3,8] · David M. Smadja[1,2,3]

Published online: 28 September 2018

Abstract

Idiopathic pulmonary fibrosis (IPF) is a devastating lung disease characterized by fibroblast proliferation, extracellular matrix deposition, destruction of pulmonary alveolar architecture and vascular remodeling. Apart pirfenidone or nintendanib that only slow down the fibrotic process, there is no curative treatment other than lung transplantation. Because cell therapy approaches have been proposed in IPF, we hypothesized that injection of endothelial colony-forming cells (ECFCs), the vasculogenic subtype of endothelial progenitor cells, could modulate fibrosis in a Nude mouse model of bleomycin induced-pulmonary fibrosis. Mice were injected with ECFCs isolated from cord blood and from peripheral blood of adult IPF patients at two time-points: during the development of the fibrosis or once the fibrosis was constituted. We assessed morbidity, weight variation, collagen deposition, lung imaging by microCT, Fulton score and microvascular density. Neither ECFCs isolated from cord blood nor from IPF patients were able to modulate fibrosis or vascular density during fibrogenesis or when fibrosis was constituted. These findings indicate that human ECFCs do not promote an adaptive regenerative response in the lung upon fibrosis or angiogenic process in the setting of bleomycin-induced pulmonary fibrosis in Nude mice.

Keywords Endothelial progenitor cells · Endothelial colony forming cells · ECFC · Fibrosis · Lung · Bleomycin

Introduction

Idiopathic pulmonary fibrosis (IPF) is a severe, progressive and irreversible lung disease that belongs to the Usual Interstitial Pneumonias (UIP). It mainly occurs in older adults and the prognosis is poor with a median survival after diagnosis comprised between 2 and 4 years [1]. It is characterized by a histologic or radiologic pattern of UIP. The diagnosis, made by an interdisciplinary team, requires the exclusion of other known causes of interstitial lung disease and the presence of UIP pattern on high-resolution computed tomography (HRCT) or lung biopsy [2].

Although there is no curative treatment, a few selected patients can benefit from lung transplantation with a median

Electronic supplementary material The online version of this article (https://doi.org/10.1007/s12015-018-9846-5) contains supplementary material, which is available to authorized users.

✉ David M. Smadja
david.smadja@parisdescartes.fr

[1] AP-HP, European Georges Pompidou Hospital, Hematology Department , Paris, France

[2] Paris Descartes University, Sorbonne Paris Cité, Paris, France

[3] Inserm UMR-S1140, Paris, France

[4] AP-HP, Avicenne Hospital, Physiology Department , Paris, France

[5] Laboratory EA 2496 Orofacial Pathologies, Imaging and Biotherapies, Montrouge, France

[6] Pharmacogenomics Unit, Department of Genetics, Institut Curie, Paris, France

[7] Centre Chirurgical Marie Lannelongue, INSERM U999, Le Plessis Robinson, France

[8] AP-HP, European Georges Pompidou Hospital, Respiratory Medicine Department , Paris, France

survival estimated to 4.5 years [3]. Besides, the CAPACITY trial showed in 2011 a reduction in decline of forced vital capacity (FVC) in patients treated by pirfenidone. Pirfenidone is an oral antifibrotic drug with pleiotropic effects: it regulates the activity of transforming growth factor (TGF)-β and tumor necrosis factor (TNF)-α in vitro, reduces fibroblast proliferation and collagen synthesis in animal models of lung fibrosis [4]. Further, the INPULSIS trial in 2014 showed a reduction of FVC decline in patients treated by nintedanib, an intracellular inhibitor targeting multiple tyrosine kinase receptors (VEGF, FGF, PDGF) [5]. However, those two drugs do not reverse the fibrotic process and there is still a need for new therapeutic strategies.

IPF is constantly associated with a heterogeneous vascular remodeling with a rarefaction of alveolar capillaries in fibrotic areas [6]. Normalization of the lung vasculature, by improving gas exchanges, could improve the clinical course of IPF. To that aim, cell therapy is one of the currently explored options [7]. Indeed, administration of vasculogenic cells able to improve lung vasculature could be a good therapeutic option to regenerate damaged tissues and/or to reverse fibrosis [8]. Endothelial colony-forming cells (ECFCs) are a population of cells able to differentiate into endothelial cells and to form new blood vessels in adult [9]. ECFCs have already been described as dysfunctional in several pulmonary diseases such as pulmonary arterial hypertension with BMPRII mutation [10], bronchopulmonary dysplasia [11] or chronic obstructive pulmonary disease [12]. In IPF, not only circulating ECFCs are decreased but their phenotype differs during exacerbations of the disease [13].

We hypothesized that ECFC treatment could modulate IPF either improving or worsening the pathology. In this study, we studied cord-blood ECFCs as well as ECFCs from peripheral blood of IPF patients because we assumed that these two types of cells may have different effects on lung fibrosis. We compared their effects in terms of modulation of fibrosis and/or vascular lesions when injected to a preclinical model of bleomycin-induced fibrosis in Nude mice.

Material and Methods

Bleomycin-Induced Model of Lung Fibrosis in Nude Mice

All animals' experiments were performed at the Animals facilities of the faculty of Pharmacy of Paris Descartes University and approved by the Paris V ethic committee (project n° 2015041318006741). NMRI $Fox^{nu/nu}$ male mice (6–11 weeks) were purchased from Janvier Laboratories (Le Genest-Saint Isle, France). Fibrosis was induced by intratracheal injection of bleomycin (Sanofi, France) at the concentration of 3UI/g under anesthesia by a mix oxygen-isoflurane 2% as defined in preliminary experiments (doses tested: 1.5UI/g, 2UI/g, 3UI/g, 6UI/g and 12UI/g). Weight was monitored at days 3, 7, 10, 14 and 21 after injection, depending on the experiment.

Intravenous injection of ECFCs in suspension in PBS (200 μL) was performed by retro-orbital route under anesthesia by a mix oxygen-isoflurane 2%. ECFCs isolated from at least three different cord-bloods or patients were used in the experiments.

After anesthesia by pentobarbital (60 mg/kg), right lung was insufflated with 4% PFA and the left one frozen in liquid nitrogen before storage at −80 °C. The heart was also harvested and conserved in saline before dissection in order to calculate Fulton score as previously described [14].

ECFC Isolation and Culture

Human umbilical cord blood was obtained from the Cell therapy Unit of Saint-Louis Hospital (APHP, Paris). Cord-blood endothelial colony-forming cells (CB-ECFC) were isolated from the adherent mononuclear cell (MNC) fraction as previously described [15]. CB-ECFCs were then expended on fibronectin (FN)-coated plates (Merck, Germany) using EGM-2MV (Lonza, USA) supplemented with 10% fetal bovine serum (FBS) as described elsewhere [15].

IPF-ECFC Isolation and Culture

IPF-ECFCs were isolated from patients with idiopathic pulmonary fibrosis defined according to the ATS/ERS consensus [2] and included in the COFI cohort (Avicenne hospital and European hospital Georges Pompidou, APHP, Paris). This study received an approval from the Ethic committee of Ile de France II (registry number 2006–108) and all patients signed an informed consent.

IPF-ECFCs were isolated as previously described [16], expended on fibronectin (FN)-coated plates (Merck, Germany) using EGM-2MV (Lonza, USA) supplemented with 10% fetal bovine serum (FBS) and used between passages 3 to 6.

Quantification of Fibrosis by microCT

Quantification of fibrosis by microCT was performed in collaboration with the Small Animal Platform of Paris Descartes University (Lofti Slimani and Jeremy Sadoine, EA2496, Paris Descartes) as previously described [17]. Mice were anesthetized with 3–5% isoflurane in order to maintain respiratory rate above 1000 ms for X-ray microtomography (Quantum FX Caliper, 90 kV, 160 μA, theory dose received 1653 mGy, 360° rotation). Parameters studied are mean pulmonary density, ratio between functional respiratory volume

and total pulmonary volume (FRC/TV) and bronchi volume (mm^3).

Histology

After fixation in PFA 4% for 24 h, lungs were embedded in paraffin and stained with hematoxylin-eosine and Sirius Red (Olivia Bawa, Experimental Pathology, Gustave Roussy Institute). Immunohistochemistry for ERG staining (MSK090–05, Zytomed Systems, Germany) was performed on a BenchMark ULTRA system (Ventana, USA).

Histomorphometry

For each slide, three fields were photographed on Sirius Red staining (Microscope Nikon Eclipse Cis, NIS-Element): one in the most affected region and two adjacent fields. Peribronchial or perivascular areas were excluded from analysis. Area occupied by collagen was quantified by defining a threshold with NIS-Element software. Results were expressed for $1mm^2$ of analyzed surface.

Detection of Human Cells in Lung by In Situ Hybridization

After dewaxing, samples were denatured 8 min at 85 °C and Alu probes specific of human DNA (800–2845, Ventana, USA) were hybridized for 1 h at 50 °C before incubation with a biotinylated antibody anti-FITC (Jackson Immunoresearch, 200–062-037, 1/200e). Revelation was performed with detection kit ISH BlueMap XT (Ventana, USA) and slides counterstained with Red Counterstain II (Ventana, USA).

Quantification of Human mRNA in Mouse Lung

Lungs were grinned in liquid nitrogen then mixed with RNable (Eurobio, France). RNA was extracted with chloroform and precipitated with isopropanol. Reverse transcription and real-time polymerase chain reaction were performed as previously described [18, 19]. Gene primers are shown in Supplementary Table 1. Transcripts of the *TBP* gene encoding the TATA box-binding protein, with primers selected to amplify both the mouse and the human *TBP* genes (*All-TBP*), were quantified as an endogenous RNA control. Transcripts of Hs-*PPIA,* Peptidylprolyl Isomerase A, specific of human RNA, or of *ALU* were used to detect human RNA in mouse lung.

For design of the experiment (Supplementary Table 2), dilutions of known concentrations of mouse RNA (Mm) in human RNA (Hs) were performed. Transcripts specific of human or mouse *TBP* genes (Hs-*TPB* and Mm-*TBP*) and transcripts of Hs-*PPIA* and *ALU* were quantified to determine the detection limit of this technique (0,05% for *PPIA* and 0,5% for *ALU*).

Statistics

All analyses were performed with Prism software (GraphPad). Results were analyzed with non-parametric test of Mann Whitney or Kruskall-Wallis test followed by Dunn multiple comparisons post-test if there were more than two groups. P value <0.05 was considered as statistically significant. Aberrant values were identified with Dixon test and excluded from analysis.

Results

Fibrogenesis Generation in a Nude Mouse Model of Bleomycin-Induced Pulmonary Fibrosis

Bleomycin doses needed to induce pulmonary fibrosis depend on mouse strain, environment and even bleomycin origin. Since the literature is scarce on bleomycin-induced pulmonary fibrosis in Nude mice [20], we first tested five increasing doses (1.5, 2, 3, 6 and 12UI/g) (Fig. 1a). First criterion analyzed was a composite one that grouped mice dead before the 14th day and those that had lost more than 20% of their initial weight (and that were consecutively sacrificed for ethical issues) (Fig. 1b). The second criterion was the variation of weight between days 0 and 14 (Fig. 1c). We also quantified collagen deposition in mouse lungs by histomorphometry (Fig. 1d).

As shown in Fig. 1b, use of the composite criterion allowed us to exclude 6 and 12 UI/g doses of bleomycin to induce fibrosis. For the other doses, we observed less than 25% mice fulfilling this criterion, a rate that we considered as acceptable. We quantified collagen deposition and observed a significant increase of collagen area only in lungs of mice receiving 3 UI/g of bleomycin. Therefore, the 3UI/g dose was chosen as the best compromise between lung fibrosis and survival rate. Furthermore, the 3UI/kg dose induced characteristic honeycomb lesions in this Nude mouse model (Fig. 1e).

Cord Blood and IPF-ECFCs Did Not Modulate Fibrogenesis

We then studied the potential effect of CB-ECFCs on lung fibrosis formation. Increasing CB-ECFC doses (10^4, 10^5 or 10^6/mouse) were administered by IV route 1 day after intratracheal 3UI/g bleomycin (Fig. 2a). Only mice that received bleomycin (BLM/mice) died or presented a major weight loss except those that received the highest dose of CB-ECFCs (Fig. 2b). For the second criterion, there was a trend toward a reduced weight loss in BLM/mice with the highest dose of CB-ECFCs compared to those that received only PBS ($p = 0.15$) (Fig. 2c).

Fulton score was calculated in order to evaluate the development of pulmonary hypertension (PH), which is a common

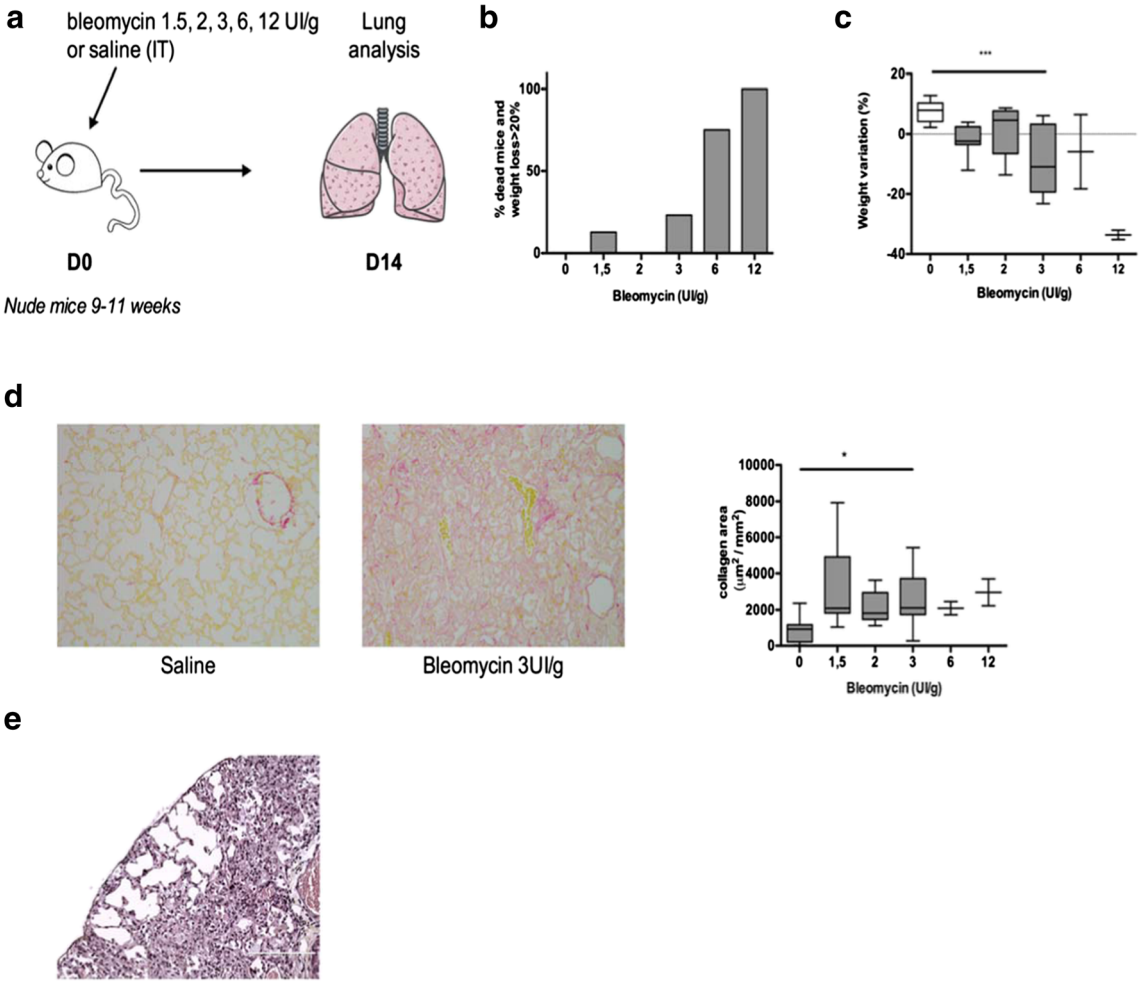

Fig. 1 Dosage testing of CB-ECFCs for modulation of fibrosis formation. a Experimental protocol ($n = 5$–13). Mice received increasing doses of bleomycin intratracheally on day 0 (1.5UI/g, 2UI/g, 3UI/g, 6UI/g and 12UI/g) and lungs were analyzed at day 14. **b** Composite criterion (percentage of dead mice and mice that lost more than 20% of initial weight). **c** Variation of weight between day 0 and 14 (%). **d** Lung histology (Red Sirius staining, objective ×40), quantification of collagen deposition by histomorphometry ($\mu m^2/mm^2$) $^*p < 0.05$ $^{**}p < 0.01$ $^{***}p < 0.005$. **e** Image of honeycombing in lung of bleomycin mice (HES objective × 40)

complication of IPF. Although not statistically significant, BLM/mice showed a median higher Fulton score than control mice, independently from CB-ECFCs administration (Fig. 2d). Regarding quantification of fibrosis by histomorphometry, we noticed a significant increased collagen accumulation in BLM/mice compared to saline/mice ($p < 0.05$). Increased collagen remained unchanged upon CB-ECFCs administration (Fig. 2e). The presence of human CB-ECFCs was further explored in mouse lungs at the end of the experiment by in situ hybridization or detection of human mRNA. Whatever the method used, either specific staining with Alu probes or quantification of human mRNAs *PPIA* or *ALU* (Supplementary Table 3), we did not evidence human CB-ECFCs in mouse lung at day 14 (data not shown).

We previously described that ECFC from IPF patients exerted different vesiculation properties than control-ECFC [16]. Thus, we tested IPF-ECFC properties on fibrogenesis in Nude mice, when administered 1 day after intratracheal bleomycin. We chose the same dose of 10^6 cells as determined for CB-ECFCs (Fig. 3a). Regarding the composite criterion (Fig. 3b), weight variation (Fig. 3c) or histological quantification of fibrosis (Fig. 3d and f), we confirmed the significant difference between saline/mice and BLM/mice that did not receive cells. However, no differences in these three parameters were noticed between groups receiving ECFCs from CB or IPF patients after bleomycin (Fig. 3b, c d and f).

We also assessed vascular density with ERG staining. Vascular density was increased in BLM/mice compared to saline/mice. Again, no modulation by either CB-ECFCs or IPF-ECFCs was observed (Fig. 3e and g).

Quantification of lung fibrosis was finally evaluated by microCT. Three parameters were studied: mean pulmonary density, ratio between respiratory functional volume and total pulmonary volume (FRC/TV) and bronchial volume (Fig. 4a–l). Regarding the two first parameters, we noticed a significant increase in BLM/mice compared to saline/mice. This reflected the

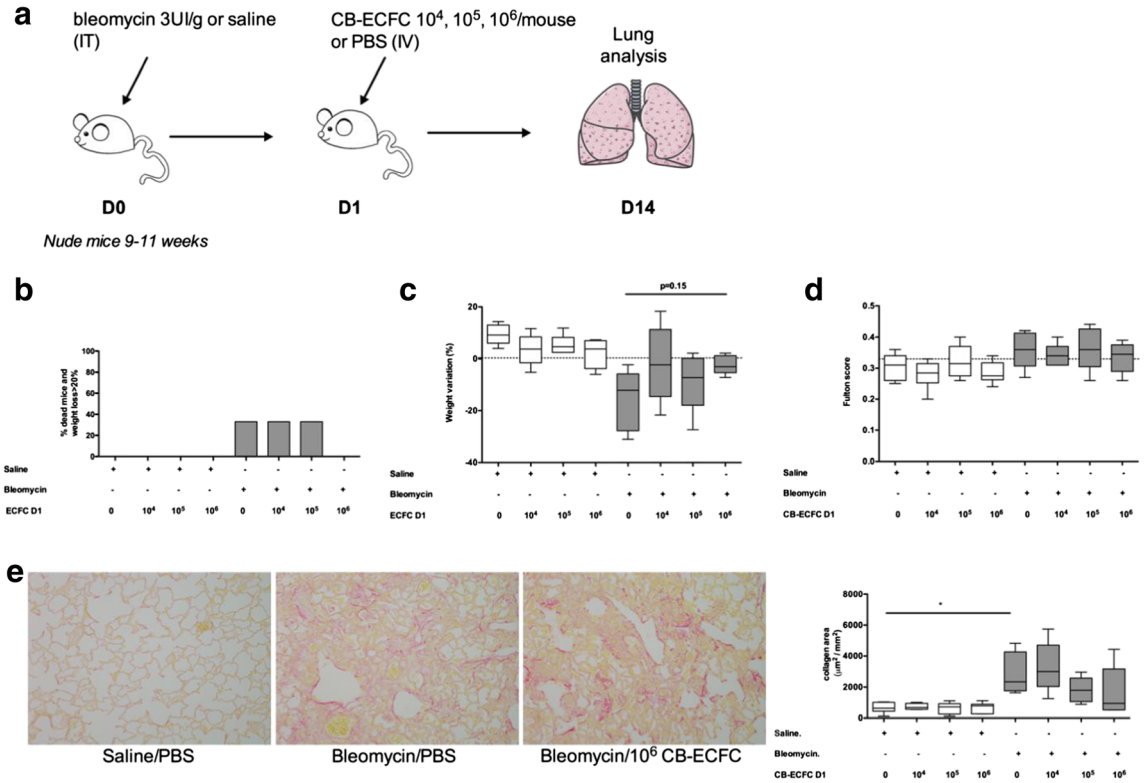

Fig. 2 Modulation of fibrosis formation by CB-ECFCs. a Experimental protocol ($n = 6$). Mice received 3 UI/g of bleomycin intratracheally on day 0 and increasing doses of CB-ECFCs (10^4, 10^5, 10^6/mouse) by IV route at D1. Lung were analyzed at day 14. **b** Composite criterion (percentage of dead mice and mice that lost more than 20% of initial weight). **c** Variation of weight between day 0 and 14 (%). **d** Fulton Score (VD/(VG + SIV)). **e** Lung histology (Red Sirius staining, objective ×40), quantification of collagen deposition by histomorphometry ($\mu m^2/mm^2$) $*p < 0.05$ $**p < 0.01$ $***p < 0.005$

fibrotic process and collagen deposition ($p < 0.01$). However, we did not notice any difference between BLM/mice groups according to ECFC injection (Fig. 4m and n). Bronchial dilation is a phenomenon described in pulmonary fibrosis and a consequence of the fibrotic process. BLM/mice thus presented bronchial dilation, significantly more than saline/mice. In this case, we did not notice any difference according to cell treatment (Fig. 4o). Last, presence of CB-ECFCs or IPF-ECFCs was explored in mouse lungs at the end of the experiment by in situ hybridization: no human cells were detectable for any of the conditions studied (Supplementary Fig. 2). Because mouse age could affect the vessel maturity and the efficiency of cell injection, we compared the effects of the injection of 10^6 CB-ECFCs in younger mice (mice aged 7 weeks vs. 11 weeks previously used). We did not find any difference of ECFC effects according to age for all the criteria studied despite an increased reactivity to bleomycin from old mice, independently of ECFC injection (Fig. 5a–f).

Modulation of Constituted Fibrosis by CB-ECFCs

In the second part of the study, CB-ECFCs were administered 14 days after intratracheal bleomycin to explore their potential effects on constituted fibrosis (Fig. 6a). Data interpretation followed the criteria described above. Mortality or important weight loss was only reported in BLM/mice (Fig. 6b). This criterion reached the level of 50% in the group of BLM/mice that received 10^5 CB-ECFCs. No significant difference in weight variation was shown between saline/mice and BLM/mice, in the presence or in the absence of CB-ECFC administration (Fig. 6c). However, Fulton score was significantly higher in BLM/mice compared to saline/mice ($p < 0.05$), but remained unchanged following CB-ECFC administration (Fig. 6d). We finally quantified fibrosis in lungs and found a significant increase in collagen accumulation in lungs of BLM/mice compared to saline/mice ($p < 0.05$), that remained unchanged after CB-ECFCs administration (Fig. 6e). Finally, we did not detect human CB-ECFCs by in situ hybridization or quantification of human mRNA (Supplementary Table 3).

Discussion

In this study, we demonstrated that vasculogenic ECFCs did not modify bleomycin-induced lung fibrosis in Nude mice. While fibrosis induced by bleomycin in this mouse model was well characterized by weight loss, histology, microCT and microvessel density, none of these parameters significantly

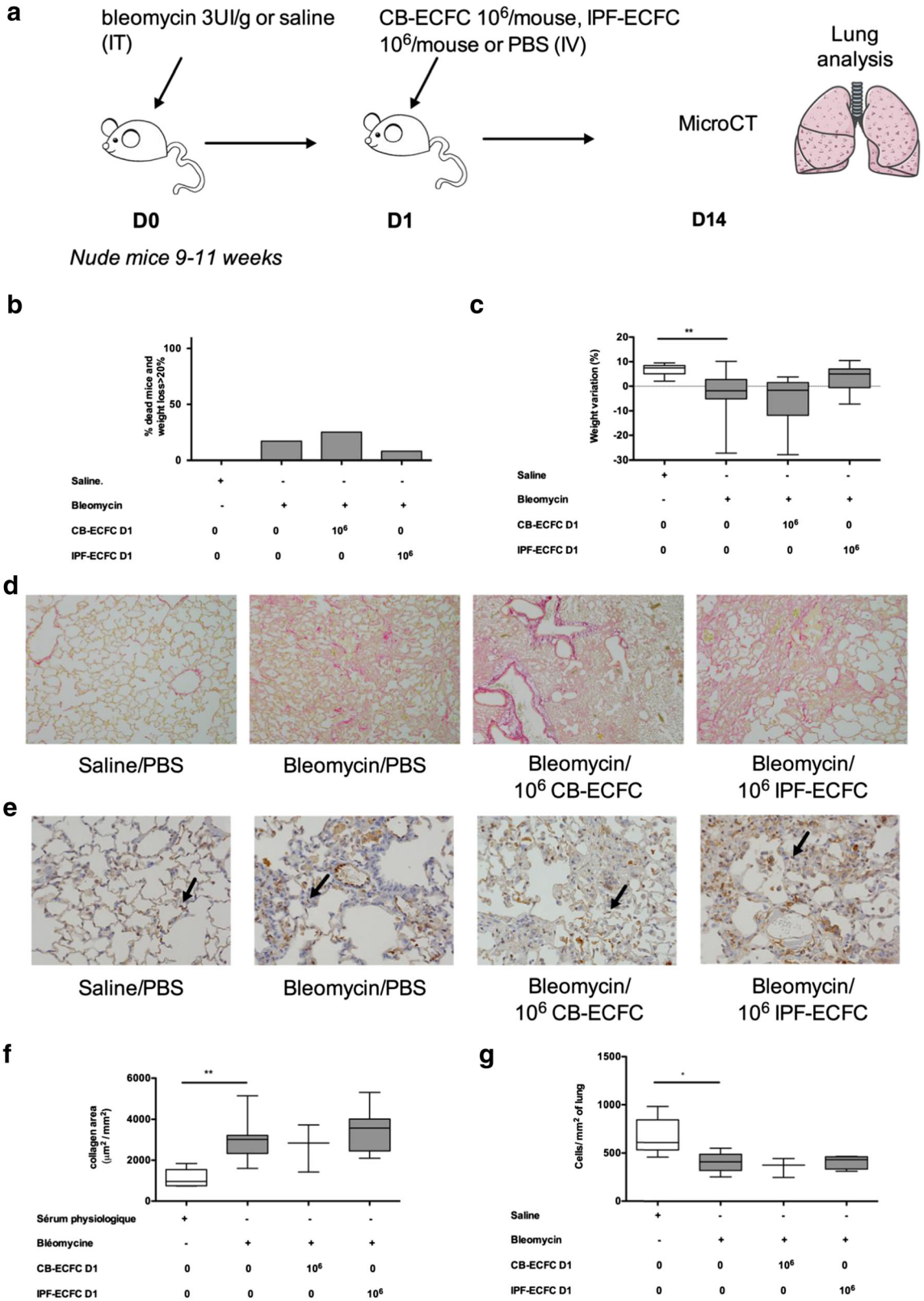

Fig. 3 Modulation of fibrosis formation by IPF-ECFCs. a Experimental protocol ($n = 12$). Mice received 3 UI/g of bleomycin intratracheally on day 0 and 10^6 CB-ECFCs or IPF-ECFC/mouse intravenously at D1. Lungs were analyzed at day 14. **b** Composite criterion (percentage of dead mice and mice that lost more than 20% of initial weight). **c** Variation of weight between day 0 and 14 (%). **d** Lung histology (Red Sirius staining, objective ×40). **e** Vascular density (ERG staining, arrow, objective ×40). **f** Quantification of collagen deposition by histomorphometry ($\mu m^2/mm^2$). **g** Quantification of vascular density (ERG positive cells/mm^2) $*p < 0.05$ $**p < 0.01$ $***p < 0.005$

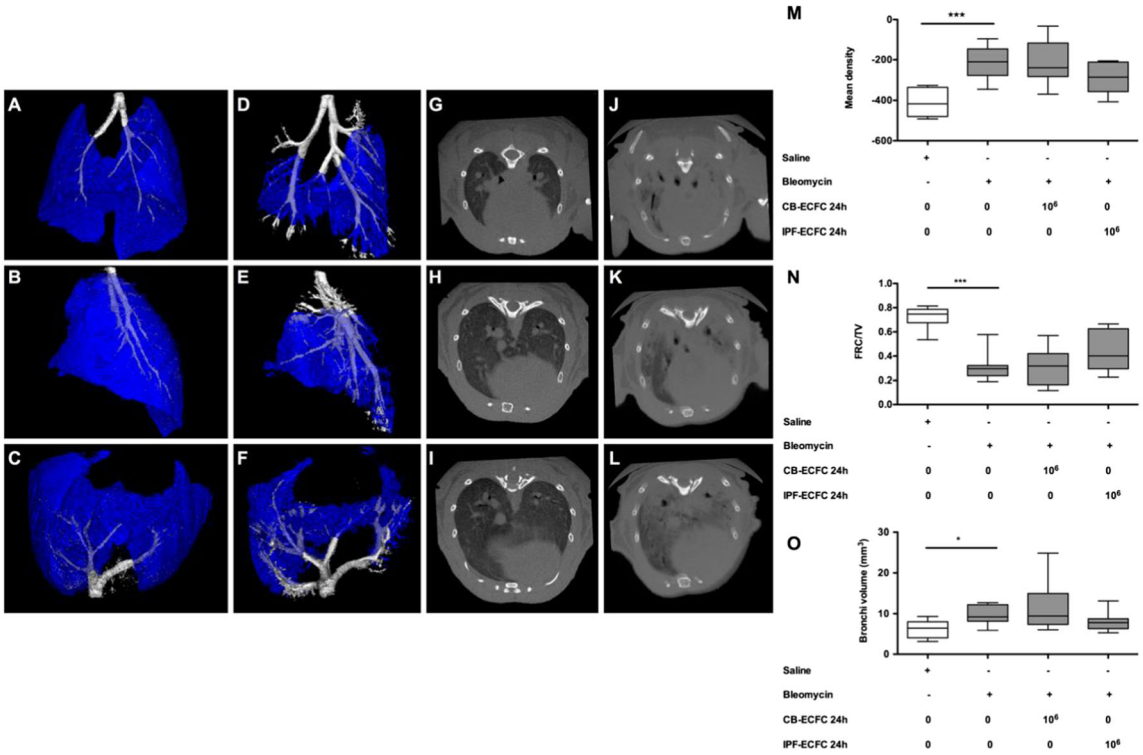

Fig. 4 Evaluation of lung fibrosis by microCT. Volumetric representation of bronchial tree (white) and functional respiratory volume (blue): frontal (**a**), sagittal (**b**) and transversal (**c**) view of saline mice and frontal (**d**), sagittal (**e**) and transversal (**f**) view of bleomycin mice (administration of 3 UI/g of bleomycin intratracheally on day 0). Visualization of 3 transversal view of pulmonary parenchyma: saline mice (**g**, **h**, **i**) and bleomycin mice (**j**, **k**, **l**). **m** Mean pulmonary density. N. Ratio between functional respiratory volume and total pulmonary volume (FRC/TV) O. Bronchi volume (mm^3) $*p < 0.05$ $**p < 0.01$ $***p < 0.005$

improved after ECFC administration by IV route, either at one or 14 days after bleomycin intratracheal administration.

We hypothesized that healthy or IPF patients' ECFCs could have a beneficial or deleterious effect in lung fibrosis since endothelial lesions are always observed during IPF [21, 22]. The phenotype of pulmonary vascular endothelial cells is disrupted in IPF with an increase of proliferation and apoptosis marker expression [6, 23], and this is associated with an imbalance between circulating markers of endothelial activation and regeneration [13, 24]. In addition, ECFCs are of medullary origin and cells mobilized from bone-marrow are known to home to the lungs during early phases of the disease in a bleomycin-induced pulmonary model [25].

However, neither "healthy" ECFCs from CB nor from IPF patients modified lung fibrosis in the preclinical model used. We evaluated first the effect of injection of CB-ECFCs in this model. We firstly focused on fibrosis formation with ECFCs injection 1 day after bleomycin administration. In BLM/mice receiving 10^6 ECFCs, we found no effect of cell injection on collagen deposition or PH development. As one of the hypotheses of this work was that IPF-ECFCs might be dysfunctional and play a role in IPF physiopathology, we also tested the effects of IPF-ECFCs in this model. The objective was to compare the angiogenic and fibrotic potential of IPF-ECFCs to control ECFCs. Here, after IV injection of IPF-ECFCs or control CB-ECFCs, we did not find any significant difference neither in weight variation, nor in lung fibrosis development. We also compared quantification of micro-vascular density in bleomycin-induced fibrosis in mice. Micro-vascular density was increased in BLM/mice, data in favor of the development of vascular abnormalities in our model but again it was not modulated by the administration of cells whatever CB or IPF origin. This result is in accordance with the Fulton score that increased in BLM/mice, as reflected by the development of PH in line with a vascular damage. We finally injected ECFCs 14 days after bleomycin instillation, when fibrosis was already constituted. We did not observe any effect of cells on mouse weight whatever the quantity of ECFCs injected. Fulton score was significantly increased in mice that received bleomycin compared to controls, but did not improve following cell therapy.

This absence of effects of cell therapy on lung fibrosis needs to be discussed regarding our preclinical model. Bleomycin-induced lung fibrosis is currently the best-characterized model. After an intra-tracheal injection of

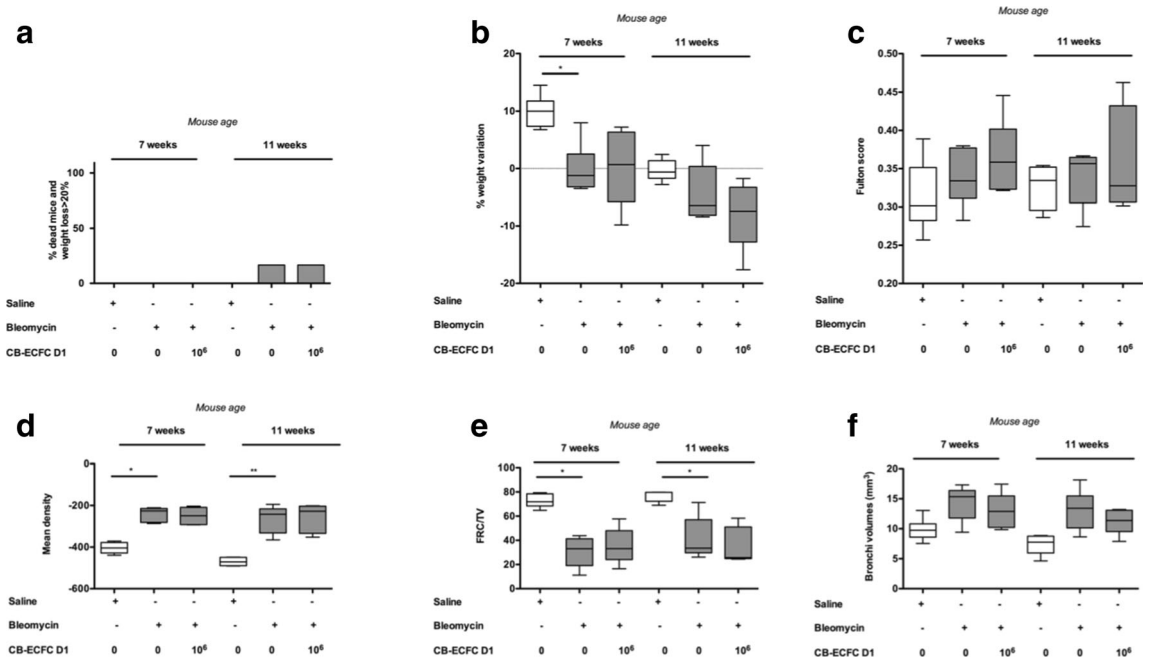

Fig. 5 Effect on mouse age on the modulation of fibrosis formation by CB-ECFCs (mice aged 7 weeks and 11 weeks) ($N = 5$). **a** Composite criterion (percentage of dead mice and mice that lost more than 20% of initial weight). **b** Variation of weight between day 0 and 14 (%). **c** Fulton Score (VD/(VG + SIV)). Evaluation of lung fibrosis by microCT **d** Mean pulmonary density. **e** Ratio between functional respiratory volume and total pulmonary volume (FRC/TV) **f** Bronchi volume (mm^3) $*p < 0.05$ $**p < 0.01$ $***p < 0.005$

bleomycin, a one-week inflammatory period precedes the development of lung fibrosis. After 1 month, fibrosis began to regress even if studies have shown that it can persist up to 60–90 days [26]. Bleomycin response depends notably on mouse strain, most studies using C57Bl/6 or SCID-beige. To test the effects of human cells in this model, we chose the Nude mouse strain for which a huge amount of data evidenced the formation of new vessels following ECFC cell-therapy for post-ischemic revascularization [27, 28]. This strain, although not usually used to study fibrosis [20], proved robustness according to our present data and probably better reproduces human disease since we observed the presence of honeycomb lesions (Fig. 1e), a pathognomonic sign of human IPF rarely observed in murine models. Moreover, animals that received bleomycin had an increased Fulton score compared to saline controls. This is consistent with the development of PH secondary to lung fibrosis and confirms the relevance of our in vivo model. However, we did not find any difference of CB-ECFCs or IPF-ECFCs on the modulation of lung fibrosis. Other authors described equivalent in vivo vasculogenic potential of ECFC despite significant in vitro differences [29]. Indeed, our group and others described that adult ECFCs from healthy donors and CB-ECFCs have different vasculogenic ability [30, 31]. In this bleomycin-induced fibrosis model, the aim of vasculogenic cell therapy was to improve oxygenation of the lung, therefore decreasing fibrogenesis. We did not found any significant effect of ECFCs on lung fibrosis whatever the time-point of cell administration. Interestingly, IPF-ECFCs did not show either a deleterious effect on fibrogenesis despite their potential proapoptotic or senescent phenotype [12, 32], or as we previously showed, an ability to secrete fibrinolytic microvesicles favoring fibroblast migration [16]. Therefore, this discrepancy between in vitro and in vivo potential allows us to propose ECFCs in IPF as a “liquid biopsy” biomarker rather than an autologous cell therapy product. Nude mouse model has been used to test the efficacy of embryonic mesenchymal stem cells [20]. Even if discrepant results have been provided, numerous studies have attested the efficacy of MSC in murine models of lung fibrosis in strains others than Nude [33]. The positive effect of MSCs is probably related to their paracrine effect [34, 35]. However, MSCs could also induce a worsening of fibrosis because of incorporation in fibrotic area, but we did not explore MSC effects in our model. Regarding ECFCs, they have been described to adopt a mesenchymal phenotype via an endothelial-to-mesenchymal transition stimulated by TGF-β1 [36]. Because TGF-β1 is the main cytokine present in fibrotic lung, this could happen after ECFCs injection. However, our data show that ECFCs did not induce a worsening of either fibrogenesis or constituted fibrosis.

Finally, it was shown that mouse age could modify their sensibility to fibrosis development and to a potential treatment [37]. In consequence, we compared the effects of injection of CB-ECFCs on lung fibrosis development in mice aged of 7 weeks or 11 weeks. Even if younger mice were a little less responsive to

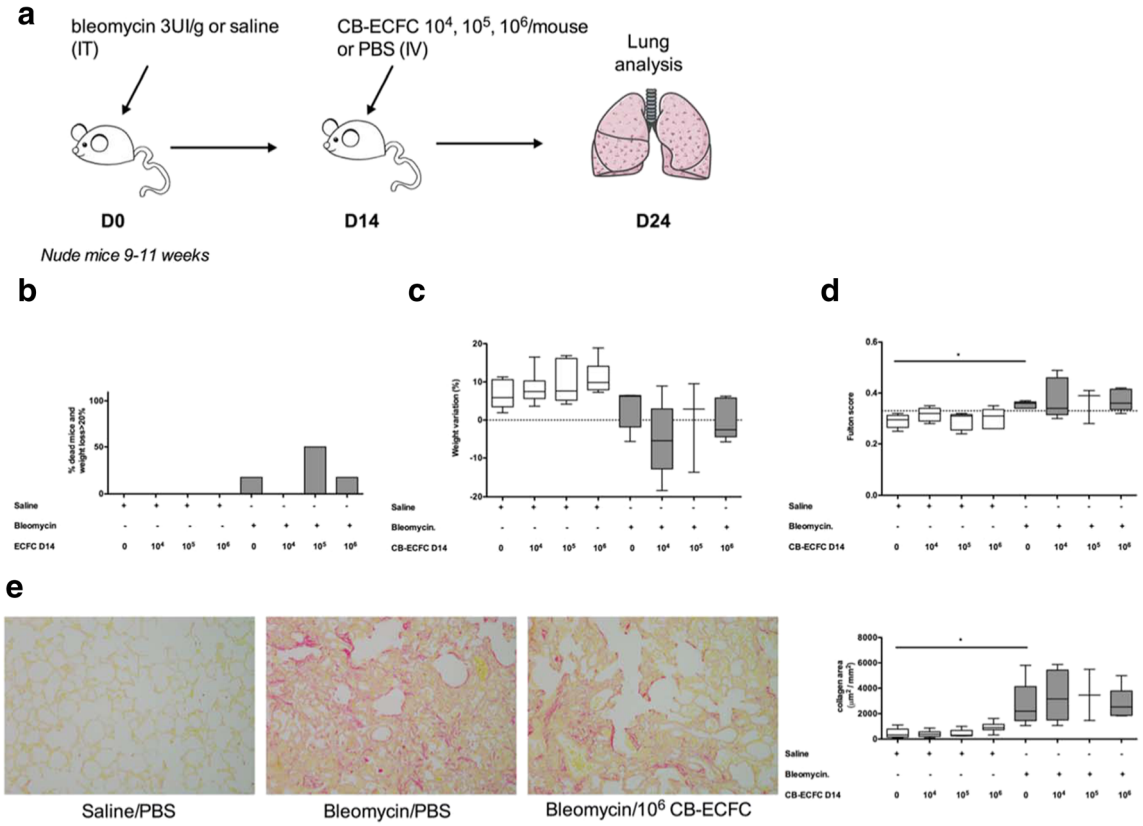

Fig. 6 Modulation of constituted fibrosis by CB-ECFCs. a Experimental protocol ($n = 6$). Mice received 3 UI/g of bleomycin intratracheally on day 0 and increasing doses of CB-ECFCs (10^4, 10^5, 10^6 /mouse) intravenously at day 14. Lung were analyzed at day 24. **b** Composite criterion (percentage of dead mice and mice that lost more than 20% of initial weight). **c** Variation of weight between day 0 and 24 (%). **d** Fulton Score (VD/(VG + SIV)). **e** Lung histology (Red Sirius staining, objective x40), quantification of collagen deposition by histomorphometry ($\mu m^2/mm^2$) $*p < 0.05$ $**p < 0.01$ $***p < 0.005$

bleomycin (trends to decrease of mortality and of loss of weight), CB-ECFCs did not improve fibrosis development.

Importantly, we did not find any human ECFCs in mouse lungs by quantitative RT-qPCR on total lung RNA or by in situ hybridization. We and others have shown that ECFCs have a tropism toward lung during the first 48 h after injection in Nude mice [38, 39]. This result makes us reconsidering the assumption that ECFCs would incorporate into lung vasculature to form new vessels. This result is in accordance with results of most stem cell therapy approaches in heart or retina diseases [40, 41].

To conclude, in this work we developed a reliable preclinical model of bleomycin–induced fibrosis in Nude mice. We explored the potential of ECFCs isolated from cord-blood or peripheral blood from IPF patients to modulate mouse lung fibrogenesis and vasculature abnormalities. Negative results argue against a potential benefit of vasculogenic cell therapy in the pathogenesis of IPF.

Acknowledgments We thank the animal Platform, CRP2 – UMS 3612 CNRS – US25 Inserm-IRD – Faculté de Pharmacie de Paris, Université Paris Descartes, Paris, France.

We are indebted to cell therapy department of Saint Louis Hospital (AP-HP, Paris) for cord blood samples. We thank Anna Lokajczyk and Nathalie Nevo for providing ECFCs from cord-blood.

This work was supported by grants of the Chancellerie des Universités (Legs Poix), PRES and PROMEX STIFTUNG FUR DIE FORSCHUNG foundation.

A. Blandinieres was supported by grants from AP-HP and INSERM (contrat d'accueil).

Compliance with Ethical Standards

Conflict of Interest Authors do not have any conflict of interest to declare.

References

1. Lederer, D. J., & Martinez, F. J. (2018). Idiopathic pulmonary fibrosis. *The New England Journal of Medicine, 378*(19), 1811–1823.
2. Raghu, G., Collard, H. R., Egan, J. J., Martinez, F. J., Behr, J., Brown, K. K., Colby, T. V., Cordier, J. F., Flaherty, K. R., Lasky, J. A., Lynch, D. A., Ryu, J. H., Swigris, J. J., Wells, A. U., Ancochea, J., Bouros, D., Carvalho, C., Costabel, U., Ebina, M., Hansell, D. M., Johkoh, T., Kim, D. S., King te Jr, Kondoh, Y., Myers, J., Müller, N. L.,

Nicholson, A. G., Richeldi, L., Selman, M., Dudden, R. F., Griss, B. S., Protzko, S. L., Schünemann, H. J., & ATS/ERS/JRS/ALAT Committee on Idiopathic Pulmonary Fibrosis. (2011). An official ATS/ERS/JRS/ALAT statement: idiopathic pulmonary fibrosis: evidence-based guidelines for diagnosis and management. *American Journal of Respiratory and Critical Care Medicine, 183*(6), 788–824.

3. Kistler, K. D., Nalysnyk, L., Rotella, P., & Esser, D. (2014). Lung transplantation in idiopathic pulmonary fibrosis: a systematic review of the literature. *BMC Pulmonary Medicine, 14*, 139.
4. Noble, P. W., Albera, C., Bradford, W. Z., Costabel, U., Glassberg, M. K., Kardatzke, D., King Jr., T. E., Lancaster, L., Sahn, S. A., Szwarcberg, J., Valeyre, D., & du Bois, R. M. (2011). Pirfenidone in patients with idiopathic pulmonary fibrosis (CAPACITY): two randomised trials. *The Lancet, 377*(9779), 1760–1769.
5. Richeldi, L., du Bois, R. M., Raghu, G., Azuma, A., Brown, K. K., Costabel, U., Cottin, V., Flaherty, K. R., Hansell, D. M., Inoue, Y., Kim, D. S., Kolb, M., Nicholson, A. G., Noble, P. W., Selman, M., Taniguchi, H., Brun, M., le Maulf, F., Girard, M., Stowasser, S., Schlenker-Herceg, R., Disse, B., Collard, H. R., & INPULSIS Trial Investigators. (2014). Efficacy and safety of nintedanib in idiopathic pulmonary fibrosis. *The New England Journal of Medicine, 370*(22), 2071–2082.
6. Ebina, M., Shimizukawa, M., Shibata, N., Kimura, Y., Suzuki, T., Endo, M., Sasano, H., Kondo, T., & Nukiwa, T. (2004). Heterogeneous increase in CD34-positive alveolar capillaries in idiopathic pulmonary fibrosis. *American Journal of Respiratory and Critical Care Medicine, 169*(11), 1203–1208.
7. Barczyk, M., Schmidt, M., & Mattoli, S. (2015). Stem cell-based therapy in idiopathic pulmonary fibrosis. *Stem Cell Reviews and Reports, 11*(4), 598–620.
8. Weiss, D. J., & Ortiz, L. A. (2013). Cell therapy trials for lung diseases: progress and cautions. *American Journal of Respiratory and Critical Care Medicine, 188*(2), 123–125.
9. Yoder, M. C., Mead, L. E., Prater, D., Krier, T. R., Mroueh, K. N., Li, F., Krasich, R., Temm, C. J., Prchal, J. T., & Ingram, D. A. (2007). Redefining endothelial progenitor cells via clonal analysis and hematopoietic stem/progenitor cell principals. *Blood, 109*(5), 1801–1809.
10. Toshner, M., Voswinckel, R., Southwood, M., al-Lamki, R., Howard, L. S. G., Marchesan, D., Yang, J., Suntharalingam, J., Soon, E., Exley, A., Stewart, S., Hecker, M., Zhu, Z., Gehling, U., Seeger, W., Pepke-Zaba, J., & Morrell, N. W. (2009). Evidence of dysfunction of endothelial progenitors in pulmonary arterial hypertension. *American Journal of Respiratory and Critical Care Medicine, 180*(8), 780–787.
11. Baker, C. D., Balasubramaniam, V., Mourani, P. M., Sontag, M. K., Black, C. P., Ryan, S. L., & Abman, S. H. (2012). Cord blood angiogenic progenitor cells are decreased in bronchopulmonary dysplasia. *The European Respiratory Journal, 40*(6), 1516–1522.
12. Paschalaki, K. E., Starke, R. D., Hu, Y., Mercado, N., Margariti, A., Gorgoulis, V. G., Randi, A. M., & Barnes, P. J. (2013). Dysfunction of endothelial progenitor cells from smokers and chronic obstructive pulmonary disease patients due to increased DNA damage and senescence. *Stem Cells, 31*(12), 2813–2826.
13. Smadja, D. M., Mauge, L., Nunes, H., d'Audigier, C., Juvin, K., Borie, R., Carton, Z., Bertil, S., Blanchard, A., Crestani, B., Valeyre, D., Gaussem, P., & Israel-Biet, D. (2013). Imbalance of circulating endothelial cells and progenitors in idiopathic pulmonary fibrosis. *Angiogenesis, 16*(1), 147–157.
14. Xu, M. H., Gong, Y. S., Su, M. S., Dai, Z. Y., Dai, S. S., Bao, S. Z., Li, N., Zheng, R. Y., He, J. C., Chen, J. F., & Wang, X. T. (2011). Absence of the adenosine A2A receptor confers pulmonary arterial hypertension and increased pulmonary vascular remodeling in mice. *Journal of Vascular Research, 48*(2), 171–183.
15. Smadja, D.M., Dorfmüller, P., Guerin, C., et al. (2014). Cooperation between human fibrocytes and endothelial colony-forming cells increases angiogenesis via the CXCR4 pathway: Thromb Haemost [Internet] 2014 [cited 2014 Aug 25];112(5). Available from: http://www.schattauer.de/index.php?id=1214&doi=10.1160/TH13-08-0711.
16. Bacha, N. C., Blandinieres, A., Rossi, E., Gendron, N., Nevo, N., Lecourt, S., Guerin, C. L., Renard, J. M., Gaussem, P., Angles-Cano, E., Boulanger, C. M., Israel-Biet, D., & Smadja, D. M. (2018). Endothelial microparticles are associated to pathogenesis of idiopathic pulmonary fibrosis. *Stem Cell Reviews, 14*(2), 223–235.
17. Elhai, M., Avouac, J., Hoffmann-Vold, A. M., Ruzehaji, N., Amiar, O., Ruiz, B., Brahiti, H., Ponsoye, M., Fréchet, M., Burgevin, A., Pezet, S., Sadoine, J., Guilbert, T., Nicco, C., Akiba, H., Heissmeyer, V., Subramaniam, A., Resnick, R., Molberg, Ø., Kahan, A., Chiocchia, G., & Allanore, Y. (2016). OX40L blockade protects against inflammation-driven fibrosis. *Proceedings of the National Academy of Sciences of the United States of America, 113*(27), E3901–E3910.
18. Bièche, I., Onody, P., Laurendeau, I., Olivi, M., Vidaud, D., Lidereau, R., & Vidaud, M. (1999). Real-time reverse transcription-PCR assay for future management of ERBB2-based clinical applications. *Clinical Chemistry, 45*(8 Pt 1), 1148–1156.
19. Smadja, D. M., Bièche, I., Helley, D., Laurendeau, I., Simonin, G., Muller, L., Aiach, M., & Gaussem, P. (2007). Increased VEGFR2 expression during human late endothelial progenitor cells expansion enhances in vitro angiogenesis with up-regulation of integrin alpha(6). *Journal of Cellular and Molecular Medicine, 11*(5), 1149–1161.
20. Qiao, W., Zhu, H., Zhou, W.-G., et al. (2013). N-acetylcysteine-pretreated human embryonic mesenchymal stem cell administration protects against bleomycin-induced lung injury. *The American Journal of the Medical Sciences, 346*(2), 113–122.
21. Yin, Q., Nan, H.-Y., Zhang, W.-H., Yan, L. F., Cui, G. B., Huang, X. F., & Wei, J. G. (2011). Pulmonary microvascular endothelial cells from bleomycin-induced rats promote the transformation and collagen synthesis of fibroblasts. *Journal of Cellular Physiology, 226*(8), 2091–2102.
22. Cao, Z., Lis, R., Ginsberg, M., Chavez, D., Shido, K., Rabbany, S. Y., Fong, G. H., Sakmar, T. P., Rafii, S., & Ding, B. S. (2016). Targeting of the pulmonary capillary vascular niche promotes lung alveolar repair and ameliorates fibrosis. *Nature Medicine, 22*(2), 154–162.
23. Tachihara, A., Jin, E., Matsuoka, T., Ghazizadeh, M., Yoshino, S., Takemura, T., D. Travis, W., & Kawanami, O. (2006). Critical roles of capillary endothelial cells for alveolar remodeling in nonspecific and usual interstitial pneumonias. *J Nippon Med Sch, 73*(4), 203–213.
24. Collard, H. R., Calfee, C. S., Wolters, P. J., Song, J. W., Hong, S. B., Brady, S., Ishizaka, A., Jones, K. D., King Jr., T. E., Matthay, M. A., & Kim, D. S. (2010). Plasma biomarker profiles in acute exacerbation of idiopathic pulmonary fibrosis. *Am J Physiol Lung Cell Mol Physiol, 299*(1), L3–L7.
25. Banerjee, E. R., & Henderson Jr., W. R. (2012). Characterization of lung stem cell niches in a mouse model of bleomycin-induced fibrosis. *Stem Cell Research & Therapy, 3*(3), 1–21.
26. Moore, B., Lawson, W. E., Oury, T. D., Sisson, T. H., Raghavendran, K., & Hogaboam, C. M. (2013). Animal models of fibrotic lung disease. *American Journal of Respiratory Cell and Molecular Biology, 49*(2), 167–179.
27. Guerin, C. L., Blandinières, A., Planquette, B., Silvestre, J. S., Israel-Biet, D., Sanchez, O., & Smadja, D. M. (2017). Very small embryonic-like stem cells are mobilized in human peripheral blood during hypoxemic COPD exacerbations and pulmonary hypertension. *Stem Cell Reviews, 13*, 561–566.

28. d'Audigier, C., Susen, S., Blandinieres, A., Mattot, V., Saubamea, B., Rossi, E., Nevo, N., Lecourt, S., Guerin, C. L., Dizier, B., Gendron, N., Caetano, B., Gaussem, P., Soncin, F., & Smadja, D. M. (2018). Egfl7 represses the vasculogenic potential of human endothelial progenitor cells. *Stem Cell Reviews and Reports, 14*(1), 82–91.
29. Solomon, I., O'Reilly, M., Ionescu, L., et al. (2016). Functional differences between placental micro- and macrovascular endothelial colony-forming cells. *Stem Cells Translational Medicine, 5*(3), 291–300.
30. Smadja, D. M., Laurendeau, I., Avignon, C., Vidaud, M., Aiach, M., & Gaussem, P. (2006). The angiopoietin pathway is modulated by PAR-1 activation on human endothelial progenitor cells. *J Thromb Haemost, 4*(9), 2051–2058.
31. Silvestre, J.-S., Smadja, D. M., & Lévy, B. I. (2013). Postischemic revascularization: from cellular and molecular mechanisms to clinical applications. *Physiological Reviews, 93*(4), 1743–1802.
32. Jablonski, R. P., Kim, S.-J., Cheresh, P., Williams, D. B., Morales-Nebreda, L., Cheng, Y., Yeldandi, A., Bhorade, S., Pardo, A., Selman, M., Ridge, K., Gius, D., Budinger, G. R. S., & Kamp, D. W. (2017). SIRT3 deficiency promotes lung fibrosis by augmenting alveolar epithelial cell mitochondrial DNA damage and apoptosis. *The FASEB Journal, 31*(6), 2520–2532.
33. Srour, N., & Thébaud, B. (2015). Mesenchymal stromal cells in animal bleomycin pulmonary fibrosis models: a systematic review. *Stem Cells Translational Medicine, 4*(12), 1500–1510.
34. Moodley, Y., Atienza, D., Manuelpillai, U., Samuel, C. S., Tchongue, J., Ilancheran, S., Boyd, R., & Trounson, A. (2009). Human umbilical cord mesenchymal stem cells reduce fibrosis of bleomycin-induced lung injury. *The American Journal of Pathology, 175*(1), 303–313.
35. Ortiz, L. A., Gambelli, F., McBride, C., Gaupp, D., Baddoo, M., Kaminski, N., & Phinney, D. G. (2003). Mesenchymal stem cell engraftment in lung is enhanced in response to bleomycin exposure and ameliorates its fibrotic effects. *Proceedings of the National Academy of Sciences of the United States of America, 100*(14), 8407–8411.
36. Díez, M., Musri, M. M., Ferrer, E., Barberà, J. A., & Peinado, V. I. (2010). Endothelial progenitor cells undergo an endothelial-to-mesenchymal transition-like process mediated by TGFbetaRI. *Cardiovascular Research, 88*(3), 502–511.
37. Jenkins, R. G., Moore, B. B., Chambers, R. C., Eickelberg, O., Königshoff, M., Kolb, M., Laurent, G. J., Nanthakumar, C. B., Olman, M. A., Pardo, A., Selman, M., Sheppard, D., Sime, P. J., Tager, A. M., Tatler, A. L., Thannickal, V. J., White, E. S., & ATS Assembly on Respiratory Cell and Molecular Biology. (2017). An official American Thoracic Society workshop report: use of animal models for the preclinical assessment of potential therapies for pulmonary fibrosis. *American Journal of Respiratory Cell and Molecular Biology, 56*(5), 667–679.
38. Alphonse, R. S., Vadivel, A., Fung, M., Shelley, W. C., Critser, P. J., Ionescu, L., O'Reilly, M., Ohls, R. K., McConaghy, S., Eaton, F., Zhong, S., Yoder, M., & Thebaud, B. (2014). Existence, functional impairment, and lung repair potential of endothelial colony-forming cells in oxygen-induced arrested alveolar growth. *Circulation, 129*(21), 2144–2157.
39. Rossi, E., Smadja, D., Goyard, C., Cras, A., Dizier, B., Bacha, N., Lokajczyk, A., Guerin, C. L., Gendron, N., Planquette, B., Mignon, V., Bernabéu, C., Sanchez, O., & Smadja, D. M. (2017). Co-injection of mesenchymal stem cells with endothelial progenitor cells accelerates muscle recovery in hind limb ischemia through an endoglin-dependent mechanism. *Thrombosis and Haemostasis, 117*(10), 1908–1918.
40. Menasché, P., Vanneaux, V., Hagège, A., Bel, A., Cholley, B., Parouchev, A., Cacciapuoti, I., al-Daccak, R., Benhamouda, N., Blons, H., Agbulut, O., Tosca, L., Trouvin, J. H., Fabreguettes, J. R., Bellamy, V., Charron, D., Tartour, E., Tachdjian, G., Desnos, M., & Larghero, J. (2018). Transplantation of human embryonic stem cell-derived cardiovascular progenitors for severe ischemic left ventricular dysfunction. *Journal of the American College of Cardiology, 71*(4), 429–438.
41. Reid, E., Guduric-Fuchs, J., O'Neill, C. L., et al. (2018). Preclinical evaluation and optimization of a cell therapy using human cord blood-derived endothelial Colony-forming cells for ischemic retinopathies. *Stem Cells Translational Medicine, 7*(1), 59–67.